

# Functional and Metabolic Effects of Adaptive Glycerol Kinase (GLPK) Mutants in *Escherichia coli*<sup>Ⓜ</sup>

Received for publication, October 17, 2010, and in revised form, May 1, 2011. Published, JBC Papers in Press, May 6, 2011, DOI 10.1074/jbc.M110.195305

M. Kenyon Applebee<sup>†1</sup>, Andrew R. Joyce<sup>‡2</sup>, Tom M. Conrad<sup>‡</sup>, Donald W. Pettigrew<sup>¶</sup>, and Bernhard Ø. Palsson<sup>§5</sup>

From the Department of<sup>†</sup>Chemistry & Biochemistry, and<sup>§</sup>Bioengineering University of California San Diego, La Jolla, California 92093 and the<sup>¶</sup>Department of Biochemistry and Biophysics, Texas A&M University, College Station, Texas 77843-2128

Herein we measure the effect of four adaptive non-synonymous mutations to the glycerol kinase (*glpK*) gene on catalytic function and regulation, to identify changes that correlate to increased fitness in glycerol media. The mutations significantly reduce affinity for the allosteric inhibitor fructose-1,6-bisphosphate (FBP) and formation of the tetramer, which are structurally related, in a manner that correlates inversely with imparted fitness during growth on glycerol, which strongly suggests that these enzymatic parameters drive growth improvement. Counterintuitively, the *glpK* mutations also increase glycerol-induced auto-catabolite repression that reduces *glpK* transcription in a manner that correlates to fitness. This suggests that increased specific GlpK activity is attenuated by negative feedback on *glpK* expression via catabolite repression, possibly to prevent methylglyoxal toxicity. We additionally report that *glpK* mutations were fixed in 47 of 50 independent glycerol-adapted lineages. By far the most frequently mutated locus (nucleotide 218) was mutated in 20 lineages, strongly suggesting this position has an elevated mutation rate. This study demonstrates that fitness correlations can be used to interrogate adaptive processes at the protein level and to identify the regulatory constraints underlying selection and improved growth.

Adaptive mutations are selected specifically because the altered genetic locus significantly effects phenotype to improve fitness in the organism's current environment. As such, discovered adaptive single nucleotide polymorphisms provide an opportunity to study modulation of significant phenotype characteristics at the finest genetic level, and to determine the underlying molecular and biochemical mechanisms that mediate dynamic genetic control of phenotype.

In this study, we examine adaptive mutations to the glycerol kinase gene (*glpK*)<sup>3</sup> that each independently improves growth on glycerol media. These mutations were acquired during 44-day adaptive evolution experiments of *Escherichia coli* on glycerol-supplemented M9 minimal medium, and were discov-

ered by whole-genome resequencing in addition to mutations to other genes (1). Glycerol kinase was the only gene that acquired a non-synonymous mutation in all five adapted lineages.

The repeated acquisition of a mutation to the same gene suggests that the mutations are selected to alleviate a specific constraint related to the gene function. This constraint could be difficult to identify because non-synonymous mutations often alter many enzyme properties, as well as other distant interactions (1, 2). However, given a set of mutations that alleviate the same constraint with varying degrees of efficacy, the property under selection should stand out because of its correlation to fitness gain.

Glycerol kinase is the rate-limiting enzyme in glycerol metabolism (3), suggesting that the mutations alleviate insufficient *in vivo* GlpK activity during growth on glycerol. In this study, the effects of four adaptive GlpK mutants are profiled (Table 1). The fitness gains imparted by these mutants have previously been carefully measured (4), but they do not correlate with previously measured increases in  $V_{max}$  (4, 5) suggesting the mutations increase *in vivo* activity by altering a different kinetic or regulatory parameter.

Glycerol kinase catalyzes the  $Mg^{2+}$ -ATP-dependent phosphorylation of glycerol to glycerol-3-phosphate (6). Its kinetics significantly diverge from Michaelis-Menten behavior due to substrate activation by ATP (7).

GlpK activity is regulated by multiple mechanisms, including allosteric inhibition by both fructose-1,6-bisphosphate (FBP) (8) and IIA<sup>Glc</sup> (the cytosolic subunit of the glucose-specific phosphotransferase system) (9, 10). These signals of glucose metabolism and uptake, respectively, inhibit GlpK activity during growth on glucose and other catabolically preferred substrates, although there is evidence that FBP inhibition is the dominant control mechanism (11).

In solution, the GlpK enzyme exists in a dimer-tetramer equilibrium that is thermodynamically and structurally coupled to FBP binding (12, 13). On one hand, the apparent dissociation constant of the dimer-tetramer reaction is dependent on the concentration of FBP. On the other, tetramer formation is required for FBP inhibition, making the apparent affinity for FBP dependent on the concentration of protein (10, 12, 14–16).

At the transcriptional level, the *glpFKX* operon is controlled by GlpR and CRP-cAMP. The *glpFKX* operon is repressed by GlpR in absence of intracellular glycerol (specific repression), though this repression is thought to be leaky since GlpK is required to produce glycerol-3-phosphate to alleviate GlpR repression. CRP-cAMP induces *glpFKX* expression when levels

<sup>\*</sup> This work was supported in whole or in part by National Institutes of Health Grant R01-GM062791-06 (to M. K. A., A. R. J., T. M. C., and B. O. P.) and Texas Agrilife Research Project TEX09208 (to D. W. P.).

<sup>Ⓜ</sup> The on-line version of this article (available at <http://www.jbc.org>) contains supplemental Tables S1–S2 and Figs. S1–S4.

<sup>1</sup> To whom correspondence should be addressed: 9500 Gilman Dr., La Jolla, CA 92093-0126. E-mail: mapplebe@ucsd.edu.

<sup>2</sup> Present address: Venebio, 7400 Beaufont Springs Dr., Suite 300, Richmond, VA 23225.

<sup>3</sup> The abbreviations used are: *glpK*, glycerol kinase gene; FBP, fructose-1,6-bisphosphate; GLPK, glycerol kinase.

of cAMP are high and is considered necessary for strong expression as this operon is otherwise considered catabolite repressed.

## EXPERIMENTAL PROCEDURES

### *E. coli* Strains

All strains utilized in this study are derived from *E. coli* K-12 MG1655 (ATCC 47076), with the exception of those used for vector maintenance and protein expression described below. "Wild type" *E. coli* refers to genetically-unmodified MG1655 (ATCC 47076) stock strain. The GlpK mutant strains were derived in a previous study by introducing individual *glpK* mutations into the wild-type genome by  $\lambda^{\text{red}}$  recombination (5, 17).

### Purification of Mutant Glycerol Kinase Enzymes (GlpK)

**Cloning into pGEX-6P-1**—Mutant and wild-type *glpK* sequences were cloned into vector pGEX-6P-1 (GE Healthcare) using the EcoRI and XhoI restriction sites. The mutant GlpK sequences were amplified by PCR from glycerol-evolved end point colonies (supplemental Table S1) (5), and validated by Sanger sequencing. It should be noted that the EcoRI restriction site is eight codons downstream from the PreScission protease cleavage site, which adds 8 residues (Gly-Pro-Leu-Gly-Ser-Pro-Glu-Phe-) to the N terminus of the expressed protein.

**GlpK Overexpression**—Mutant GlpK proteins were expressed from pGEX-6P-1 constructs transformed into One Shot BL21 star (DE3) *E. coli* (Invitrogen). Clones were grown in  $2 \times 200$  ml cultures of LB ampicillin (100  $\mu\text{g}/\text{ml}$ ). Expression of GlpK mutants after addition of 1 mM IPTG was monitored by the 56 kDa band from SDS-PAGE analysis of whole lysate, visualized using SimplyBlue Safe Stain (Invitrogen). Optimal expression after IPTG addition was observed after 5 h.

**GlpK Purification**—Collected cells were lysed using lysozyme and sonication. GST-tagged GlpK enzymes were purified using 1 ml GSTrap FF columns (GE Healthcare). Before column loading, the sonicated lysate was clarified by centrifugation and filtration of the supernatant through a 0.45  $\mu\text{m}$  syringe filter. GSTrap FF columns were used as described by the manufacturer except that 10 mM glycerol was added to both the binding buffer and the PreScission cleavage buffer to stabilize GlpK conformation, and 2 mM  $\beta$ -mercaptoethanol was added to the binding buffer to minimize oxidative damage. Glycerol kinase protein was eluted from the column by cleavage of the glutathione *S*-transferase domain by PreScission protease (GE Healthcare). SDS-PAGE of 10 mg the eluted protein showed a high concentration of  $\sim 60$  kDa protein corresponding to GlpK, and traces of three other unknown proteins that correspond to frequently co-purified chaperones (supplemental Fig. S1).

**Gel-Permeation Chromatography**—The apparent molecular weight of each GlpK allozyme was determined by small zone analytical gel permeation chromatography using an Akta Purifier HPLC system with a Bio-Gel 0.5 m column ( $1.0 \times 30$  cm). The column was equilibrated with standard buffer (0.1 M triethanolamine-HCl, pH 7.0, 2 mM glycerol, 1 mM EDTA, 1 mM  $\beta$ -mercaptoethanol), and calibrated as previously described (15). The column was injected with 0.1 mg of each variant pro-

tein in 0.2 ml of standard buffer, with a column flow rate of 0.25 ml/min. The apparent elution volume was determined by monitoring the absorbance at 280 nm, and the apparent molecular weight was estimated by using the column calibration curve.

### Kinetic Assays

The enzymes were equilibrated with standard buffer by gel permeation chromatography. Enzyme concentrations and glycerol kinase activities at pH 7.0 and 25 °C were determined and catalytic and allosteric parameters were obtained from fits of initial-velocity enzyme kinetics data as described (18). Enzyme was assayed at 0.5  $\mu\text{g}/\text{ml}$  concentration, unless otherwise noted. Glycerol was 2 mM in all assays. ATP was 2.5 mM for studies of FBP and IIA<sup>Glc</sup> inhibition. The results are presented as the best fit parameter  $\pm$  S.E. as given from fits obtained with Kaleidagraph v. 3.51 (Synergy Software), unless otherwise noted.

Inhibition by FBP was analyzed by fitting the dependence of the specific activity (SA) on FBP concentration in Equation 1,

$$SA = SA_0 - ((SA_0(1 - W)[\text{FBP}]^{nH}) / ((K_{0.5})^{nH} + [\text{FBP}]^{nH})) \quad (\text{Eq. 1})$$

where SA refers to the SA at the indicated concentration of FBP,  $SA_0$  is the SA at 0 FBP,  $W$  is  $SA_\infty/SA_0$  with  $SA_\infty$  the SA in the saturating presence of FBP,  $K_{0.5}$  is the FBP concentration that gives one-half maximal inhibition, and  $nH$  is the Hill coefficient. The inhibition parameters could not be independently estimated from fitting the data because the apparent FBP affinities were reduced so dramatically (see "Results"). To enable data for the variant enzymes to be fitted, the values for the Hill coefficient and  $W$  were fixed to the values obtained from the fits to the N-terminal extension native enzyme.

Inhibition by IIA<sup>Glc</sup> was analyzed by fitting the dependence of the SA on the concentration of IIA<sup>Glc</sup> in Equation 2,

$$SA = SA_0 - ((SA_0(1 - W)[\text{IIA}^{\text{Glc}}]) / (K_{0.5} + [\text{IIA}^{\text{Glc}}])) \quad (\text{Eq. 2})$$

where SA is the SA at the indicated concentration of IIA<sup>Glc</sup>,  $SA_0$  is the SA at 0 IIA<sup>Glc</sup>,  $W$  is  $SA_\infty/SA_0$  with  $SA_\infty$  the SA in the saturating presence of IIA<sup>Glc</sup>, and  $K_{0.5}$  is the IIA<sup>Glc</sup> concentration that gives one-half maximal inhibition.

### Growth Rate Measurements

Each culture was grown in 200–250 ml of M9 medium + 0.2% of carbon source in a 500-ml Erlenmeyer flask incubated at 30 °C by water bath and aerated by magnetic stir bar spinning at 1200–1400 rpm. The  $A_{600}$  of the cultures were measured every 40–80 min using a Thermo Spectronic BioMate3 spectrophotometer starting at  $\sim 0.02$  *A* culture density. At least three data points (linear fit  $R^2 > 0.99$ ) were used to calculate each growth rate measurement, and the growth rate of each strain in each condition was measured on at least three different days.

### Intracellular cAMP Assays

Samples of culture were collected during logarithmic growth at absorbances between 0.10–0.30, absorbance measured at

## Functional Effects of Adaptive GLPK Mutants in *E. coli*

**TABLE 1**  
Description of examined adaptive GlpK mutants

GlpK residue change <sup>a</sup>	<i>glpK</i> genetic locus	Glycerol-adapted lineage of origin <sup>b</sup>	Effected GlpK domain	Relative fitness rank <sup>c</sup>	Growth rate of mutation strain <sup>d</sup>	Selection rate over wild type <sup>e</sup>
					$h^{-1}$	$\times 10^{-2} h^{-1}$
V61L	g184t	GC	Tetramer formation surface	1	$0.326 \pm 0.028$	$10.07 \pm 0.90$
D72V	a218t	GA & GB	Tetramer formation surface/FBP binding site	2	$0.334 \pm 0.026$	$9.82 \pm 1.03$
M271I	g816a	GD	Conserved ATPase core domain II	3	$0.319 \pm 0.020$	$7.90 \pm 1.07$
Q37P	a113c	GE	Active site loop & Putative internal GlpR site in <i>glpK</i> <sup>e</sup>	4	$0.314 \pm 0.022$	$5.84 \pm 1.11$

<sup>a</sup> Loci of changed residues differ from their description in Ref. 5 to conform to the convention of not counting the N-terminal methionine residue cleaved during protein translation.

<sup>b</sup> Strains further described in Ref. 5.

<sup>c</sup> Based on head-to-head pair-wise competitions in Ref. 4, with calculation described under "Experimental Procedures."

<sup>d</sup> Average and standard deviation from five independent measurements. The error associated with the measurements is too large to definitively determine differences in fitness from the growth rate measurements alone, which is why selection rates calculated from direct pair-wise competitions are reported.

<sup>e</sup> Reported in Ref. 73.

600 nm. Sample preparation was modeled after that described by A. Death *et al.* (19), using Millipore® 25-mm diameter 0.45- $\mu$ m pore Triton-free nitrocellulose filters. The volume of culture passed through the filter was estimated from absorbance to contain approximately the same number of cells as 1 ml of culture with an absorbance of 1 (*i.e.* 5 ml was collected from a culture at 0.2 A). Cells on the filter were immediately washed with 10 ml of 30 °C fresh media to rinse away extracellular cAMP, and then the filter was quickly submerged in 5 ml of ice-cold 65% ethanol to quench cellular activity. The samples were immediately vortexed at the maximum setting for 5–10 s and stored at –20 °C (19). The solution was evaporated by speedvac, and the dried residue re-dissolved in the cAMP assay buffer provided with the cAMP Direct Biotrack EIA kit (GE Healthcare), which was used to assay cAMP levels using the manufacturer's instructions for the non-acetylation protocol. One-fifth of each sample was used per assay. Each strain was cultured in triplicate, and each sample was assayed twice.

### Quantitative PCR

Three independent cultures of each strain were harvested during exponential growth. As described elsewhere (20, 21), RNA was isolated using Qiagen RNeasy Protect and RNeasy kit and 10  $\mu$ g of RNA was converted to cDNA using random hexamers and Invitrogen SuperScript II reverse transcriptase. Each quantitative PCR (qPCR) reaction contained 5–10 ng of cDNA, 0.3  $\mu$ M of each primer, and 12.5  $\mu$ l of 2 $\times$  SYBR Master Mix (Qiagen) (see supplemental Table S1 for primer sequences). Assays were measured by an iCycler iQ (Bio-Rad). Each qPCR reaction was performed in triplicate. The relative expression of each gene was calculated by normalization to the quantity of *dmsA* (assay for *glpK* in strain kA and kC *versus* wild type) or *rrsB* (all other assays).

qPCR results were analyzed using qGene software (22). The efficiency of each primer pair was calculated by generating a standard curve from qPCR of *E. coli* genomic DNA diluted 10<sup>2</sup>–10<sup>6</sup>-fold. Three technical replicates of each biological cDNA sample were assayed, and the C<sub>q</sub> values averaged to calculate the mean normalized expression.

### Statistical Analysis

Significant differences in growth rates, intracellular cAMP, and gene expression between each mutant strain and wild type in each growth condition were determined by one-way

ANOVA with matching of co-acquired measurements, and Dunnett's multiple comparisons post-test against wild type values. These analyses were performed on GraphPad Prism software.

Pearson correlation coefficients were calculated with two-tails using GraphPad software. The fitness differences between wild type and the *glpK* mutant strains were not measured during the previous competition study (4), so the selection rate between wild type and the Q37P mutant was estimated from the measured growth rate difference between the strains ( $0.058 h^{-1} \pm 0.016$  (S.E.), from Table 1). A single relative fitness value for each mutant strain relative to the Q37P mutant was calculated from the pool of pair-wise competition measurements (4) by averaging all possible combinations of competitions that produce an estimated fitness difference between a particular pair when summed.

### Laboratory Evolution of Additional Glycerol-adapted Strains

A total of 50 lineages were adaptively evolved on glycerol minimal medium to sample the variety of adaptive glycerol kinase mutations that may be acquired. Adaptation of lineages G1, G2, and GA-GE have been described elsewhere (1, 5, 23), and the same method was used to develop the additional 44 "eBOP" lineages. The lineages were evolved for 25 or 40 days (supplemental Table S2). Mutations to the *glpK* gene were identified by Sanger sequencing of PCR products with two sets of primers that amplify overlapping regions of the *glpK* gene, covering the region –100 bp upstream to 1,510 bp downstream of the transcription start site.

## RESULTS

**Mutant Glycerol Kinase Catalytic and Allosteric Properties**—We measured the functional properties of each of four GlpK allozymes (Table 1), including initial velocity kinetics and sensitivity to allosteric inhibitors FBP and IIA<sup>Glc</sup>, to assess the relationship between changes to enzyme function and fitness caused by the mutations. Results of these assays are shown in Fig. 1 and Table 2. The effect of the N-terminal extension is summarized in Table 2 and supplemental Note S1 and was determined not to be significant.

**Initial Velocity Catalytic Parameters**—Native GlpK has two apparent Michaelis constants that describe how the initial velocity depends on ATP concentration, a high affinity constant of about 10  $\mu$ M, and a lower affinity constant of about 2



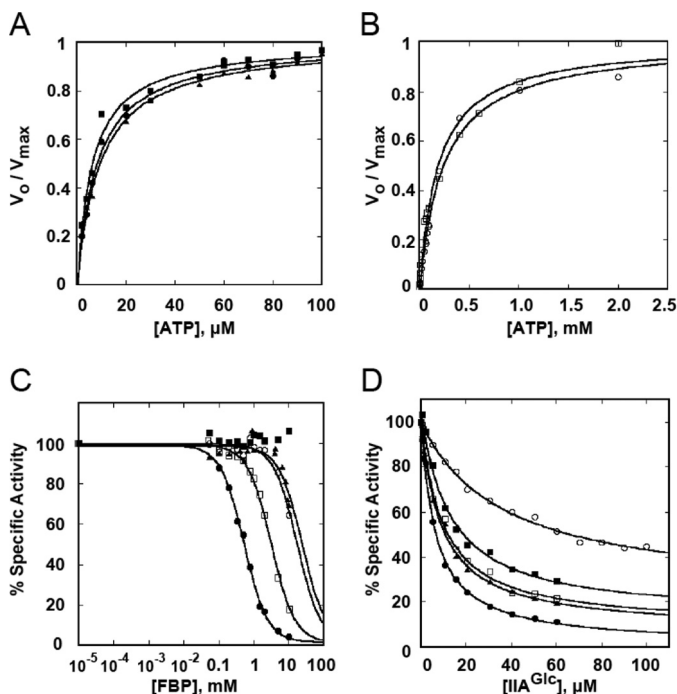


**FIGURE 1. Kinetics of GlpK mutants.** *A* and *B*, plot the dependence of the initial velocity ( $v_o$ ) of each GlpK variant on the concentration of ATP. The initial velocities have been normalized to the  $V_{max}$  for each enzyme. The lines trace the fit of the data to the Michaelis-Menten equation. The values for  $V_{max}$  and  $K_{m-ATP}$  derived from this fit are shown in Table 2. *C*, FBP inhibition. The specific activity of each variant is shown at different concentrations of FBP. Specific activities (SA) were normalized based on the specific activity ( $SA_0$ ) of each enzyme with no FBP (100%). The lines show how the data were fitted to the equation modeling FBP inhibition (Eq. 1). The V61I mutant is not appreciably inhibited by FBP so its data could not be fit to the equation; however, simulations using different values of  $K_{0.5}$  suggest that it must be greater than 100 mM.  $SA_0$  and parameters from the fits are shown in Table 2. *D*, IIA<sup>Glc</sup> inhibition. The points show the specific activity (SA) at the indicated concentration of IIA<sup>Glc</sup> normalized to the specific activity at 0 IIA<sup>Glc</sup>. The lines show the fit to the equation that models IIA<sup>Glc</sup> inhibition (Eq. 2). Values for  $SA_0$  and parameters from the fits are shown in Table 2. Symbols for GlpK allozymes: wild type: filled circle, V61I: filled square, D72V: filled triangle, M271I: open circle, Q37P: open square.

mM (7). Estimating the apparent lower ATP affinity constant is problematic because GlpK also becomes substrate-inhibited by ATP at those concentrations. For this reason, we only examined the effect of the amino acid substitutions on catalytic parameters  $K_m$  and  $V_{max}$  at ATP concentrations that reveal changes to the high affinity constant. Results of these determinations show that the catalytic properties for the GlpK allozymes V61I and D72V differ little from those of the wild type GlpK. For allozymes M271I and Q37P, both  $K_m$  for ATP and  $V_{max}$  are increased. It is evident that the increased fitness observed across the GlpK mutant strains is not correlated with their catalytic properties, as shown by the poor associated Spearman correlations (Table 2).

**Allosteric Inhibition**—Allosteric inhibition of GlpK by FBP or IIA<sup>Glc</sup> was determined in the saturating presence of glycerol (2 mM) and near-saturating ATP (2.5 mM). When assayed under these conditions in the absence of the allosteric inhibitors, all of the GlpK allozymes show similar specific activity ( $SA_0$ , Table 2). This differs from the strong effects the mutants had on  $V_{max}$  in the initial-velocity studies because the activity in these assays is largely affected by the low affinity site for ATP.

Each of the fitness improving GlpK variants reduces the apparent affinity ( $K_{0.5}$ ) for the allosteric inhibitor FBP, as shown in Fig. 1C and Table 2. The V61I variant's FBP sensitivity was most dramatically altered, lacking any appreciable inhibition even at 10 mM FBP, but higher concentrations of FBP were not evaluated because of its weak binding to the dimer that reverses the inhibition (14).

The order by which the mutations increase  $K_{0.5-FBP}$  correlates directly to their respective ability to increase fitness (Spearman correlation of 1, Table 2). Fig. 2A plots  $\log_{10}$  of  $K_{0.5-FBP}$  against the estimated selection coefficient of the GlpK mutant strains over wild type, showing an approximately linear relationship (Pearson coefficient  $r = 0.91$ ,  $p = 0.03$ ).

The GlpK allozymes also reduce allosteric control by IIA<sup>Glc</sup> (Fig. 1D). By far the biggest reduction in IIA<sup>Glc</sup> inhibition is caused by the M271I residue change, which decreases affinity 3-fold and allows the enzyme to retain ~40% of its specific activity as it nears saturation with IIA<sup>Glc</sup>, compared with native GlpK which retains less than 10%. The other residue changes have significantly less impact on sensitivity to IIA<sup>Glc</sup> inhibition, and the changes do not correlate to imparted fitness gains, suggesting this parameter is not under consistent selection.

**Tetramerization**—As described in the introduction, in solution GlpK exists in a dimer-tetramer equilibrium. This equilibrium is thermodynamically coupled to FBP binding as the apparent dissociation constant of the dimer-tetramer reaction is dependent on FBP concentration, and the apparent affinity for FBP is dependent on the concentration of protein because tetramer formation is required for FBP inhibition (10, 12, 14–16). A structural basis for this interaction is indicated by the effects of residue changes (S58W, A65T) to an  $\alpha$ -helix that is a major tetramer interface, which simultaneously reduce tetramer formation in solution and abolish FBP inhibition (15, 16).

Because the examined GlpK mutants reduce FBP inhibition, their effect on tetramer-dimer equilibrium was also examined. To do so we employed small-zone analytical gel permeation chromatography as previously described (15, 16). For these experiments, 100  $\mu$ g of each GlpK allozyme contained in 0.2 ml (9  $\mu$ M subunits) was injected onto a calibrated gel permeation chromatography column. The enzyme load is eluted in about 5 ml of buffer, suggesting the enzyme concentration is diluted from 9  $\mu$ M (subunits) to 300 nM (subunits) as the sample passes through the column if uniform distribution of the enzyme in the elution volume is assumed. This reduces the protein concentration below the saturation point for tetramer formation, and the resulting apparent molecular weight will reflect the shift in the dimer-tetramer equilibrium. For interacting systems at protein concentrations that are sufficient to allow some polymerization but insufficient for saturation of the association reaction, small-zone analytical gel permeation chromatography measures an undefined average molecular weight, which lies between the molecular weights of the largest and smallest species. The dissociation constant cannot be determined using this method, but because the same protein concentration is used for each enzyme the generated apparent molecular weights can be compared. As shown from the range of measured apparent molecular weights in Table 2, this assay pro-

## Functional Effects of Adaptive GLPK Mutants in *E. coli*

**TABLE 2**  
Catalytic and allosteric properties of GlpK mutants

GlpK residue change	Catalytic parameters <sup>a</sup>			FBP inhibition <sup>b</sup>				IIAGlc inhibition <sup>b</sup>			Molecular weight <sup>c</sup>
	$V_{max}$ unit/mg	$K_m$ ATP $\mu M$	$V_{max}/K_m$ $L^* \text{ min}^{-1} \text{ mg}^{-1}$	SA <sub>0</sub> unit/mg	W	nH	$K_{0.5}$ mM	SA <sub>0</sub> unit/mg	W	$K_{0.5}$ $\mu M$	$M_p$ , app
V61L	18 ± 0.4	6 ± 0.6	3 ± 0.1	55 ± 1	NA	NA	>100	56 ± 1	0.12 ± 0.04	13 ± 2	114,000
D72V	24 ± 0.4	9 ± 1	2.7 ± 0.1	53 ± 1	0.015	1.3	21 ± 2	53 ± 1	0.07 ± 0.01	10 ± 1	138,000
M271I	77 ± 3	250 ± 20	0.31 ± 0.1	54 ± 3	0.015	1.3	16 ± 1	69 ± 1	0.23 ± 0.03	37 ± 4	ND <sup>e</sup>
Q37P	86 ± 3	190 ± 20	0.45 ± 0.1	80 ± 1	0.015	1.3	3.2 ± 0.1	80 ± 1	0.08 ± 0.03	10 ± 1	152,000
N-term <sup>d</sup>	16.2 ± 0.4	8.5 ± 0.8	1.9 ± 0.1	62 ± 1	0.015 ± 0.02	1.3 ± 0.1	0.52 ± 0.01	62 ± 1	0.01 ± 0.01	6 ± 0.6	162,000
Native GlpK	18.1 ± 0.4	7.8 ± 0.7	2.3 ± 0.1	62 ± 2	0.03 ± 0.026	1.7 ± 0.2	0.52 ± 0.04	64 ± 1	0.09 ± 0.02	6 ± 0.6	158,000
Spearman $r^e$	0.0	-0.3	0.6	-0.6			1.00	-0.6	0.5	0.6	-1.00
$p$ value							0.0167				0.0833

<sup>a</sup> Catalytic parameters are obtained from fits of the dependence of the initial velocity on [ATP] in the saturating presence of glycerol (10 mM) to the Michaelis-Menten equation. All values on chart are shown ± S.E.

<sup>b</sup> FBP and IIA<sup>Glc</sup> inhibition are determined at 2.5 mM ATP and 10 mM glycerol. SA<sub>0</sub> is the specific activity at 0 allosteric inhibitor and W is given by the ratio SA<sub>0</sub>/SA<sub>∞</sub>, where SA<sub>∞</sub> is the specific activity in the saturating presence of the inhibitor. FBP inhibition shows cooperative homotropic effects, given by the Hill coefficient, n<sub>H</sub>.  $K_{0.5}$  is the concentration of inhibitor that gives one-half of the maximum inhibition. For fits of FBP inhibition for the variant enzymes, the values for W and n<sub>H</sub> were fixed to the values obtained for the enzyme with the N-terminal extension.

<sup>c</sup> Molecular weight of oligomeric GlpK as it exists in solution was measured by gel-permeation chromatography. The apparent molecular mass of the M271I mutant could not be determined because of its non-specific interaction with the column matrix. A similar problem was encountered for the G304S mutant, which disrupts the same residue interaction (25).

<sup>d</sup> Native GlpK enzyme carrying the same N-terminal extension (Gly-Pro-Leu-Gly-Ser-Pro-Glu-Phe) as the GlpK mutant enzymes, which remains after cleavage of the GST tag used to purify the proteins (See "Experimental Procedures" and supplemental notes).

<sup>e</sup> Correlation between the measured parameters and relative fitness imparted by the mutations is estimated using the non-parametric Spearman correlation coefficient, which was applied to parameters with measured differences across the mutants. The  $p$ -value is shown if the absolute value of Spearman  $r > 0.9$ . Measurements of the N-terminal wild type GlpK protein were used to calculate the coefficients.

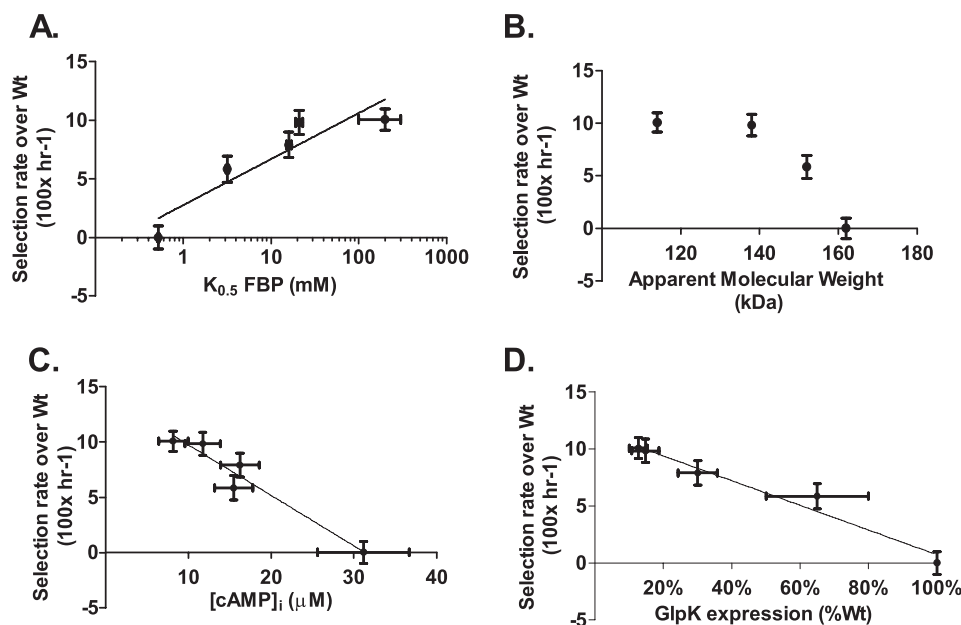


**FIGURE 2. Plots of the apparent dependence of relative fitness on (A) FBP affinity (log<sub>10</sub> transformed), (B) apparent molecular weight (an indirect measure of the tetramer dissociation constant), (C) intracellular cAMP, and (D) *glpK* expression.** Relative fitness is expressed as the approximate growth rate increase relative to wild type (h<sup>-1</sup>, × 100), calculated as described under "Experimental Procedures." No trend line is included in panel (B) because the relationship does not appear to be linear. The FBP affinity of V61L is simply estimated to be > 100 mM, but has been plotted as 150 mM ± 50 mM.

vides a quite sensitive indicator of the dissociation constant of each allozyme.

The apparent molecular weights of the assayed enzymes (Table 2) are all considerably less than that of the tetramer, 224,000, indicating that the protein has been diluted below the tetramer saturation concentration. The apparent molecular weight of the wild-type enzyme is 158,000, indicating the protein concentration used was sufficiently low to shift the dimer-tetramer equilibrium toward the dimer, and this value agrees closely with earlier work using the same column conditions (15, 16).

The apparent molecular weight of each of the fitness-improving GlpK allozymes is lower than the wild type enzyme,

indicating the amino acid substitutions shift the dimer-tetramer equilibrium of each allozyme toward the dimer. As discussed below, the sites of most of the substitutions are in the tetramer interface and are expected to perturb tetramer formation.

Similar to FBP inhibition, reduced apparent molecular weight correlates directly to increased fitness across the mutants (Fig. 2B), though this relationship is non-linear. The perfect qualitative correlation (Spearman coefficient  $r = 1$ ) is supported with a  $p$  value of 0.083, which is the most significant  $p$  value this test can provide from four data points (M271I could not be assayed due to interaction with the column matrix). This correlation indicates the amino acid substitutions progressively

**TABLE 3**  
Expression changes of catabolite regulated genes in *GlpK* mutant strains

GlpK residue change	<i>glpK</i> (repressed) <sup>a</sup>		<i>aceE</i> (activated)		<i>aspA</i> (repressed)	
	% wt expression S.D.	<i>p</i> value <sup>b</sup>	% wt expression S.D.	<i>p</i> value	% wt expression S.D.	<i>p</i> value
V61L	12.71% ± 8.13%	1.4E-04	148.90% ± 43.24%	6.6E-04	15.57% ± 4.55%	1.1E-06
D72V	14.76% ± 12.03%	1.9E-03	117.70% ± 33.06%	0.14	15.50% ± 4.24%	1.0E-06
M271I	30.75% ± 12.50%	3.6E-07	270.13% ± 204.63%	1.8E-04	25.12% ± 2.343%	4.7E-03
Q37P	65.73% ± 22.75%	2.4E-03	290.70% ± 218.60%	6.5E-05	42.48% ± 46.59%	0.12
Correlation to Relative Fitness <sup>c</sup>	-0.98	0.003	0.17	( <i>p</i> = 0.78)	-0.99	0.0005

<sup>a</sup> Indicates effect of catabolite repression on transcription of gene.

<sup>b</sup> Two-tailed one-way ANOVA with Dunnett's post-test were performed on measurements of normalized gene enrichment between wild type and *glpK*-mutant strains, assuming equal variance. Measured differences in expression that did not meet statistical significance criteria (*p* < 0.05) have been italicized.

<sup>c</sup> Correlation to relative fitness determined by calculating the Pearson coefficient between gene expression and relative strain fitness, with associated two-tailed *p* values. Correlation coefficients were calculated with wild type as a data point (100% expression).

shift the dimer-tetramer equilibrium toward the dimer, and that this effect positively impacts fitness.

The apparent molecular weight of the V61L allozyme approaches that of the dimer, indicating that tetramer formation does not appreciably occur at the protein concentrations used in gel permeation chromatography (~300 nM, subunits). This is substantially higher than the protein concentration in the initial velocity studies (9 nM, subunits), suggesting that the V61L allozyme lost sensitivity to FBP in the activity assay due to the inability to form tetramers at the assayed enzyme concentration.

The D72V and Q37P mutants also have reduced apparent molecular weight compared with the wild type enzyme, indicating these substitutions also increase the dissociation constant of the tetramer, though to less extent than V61L. This suggests that their measured increases in  $K_{0.5-FBP}$  also result from reduced tetramer formation in the assays. The correlations of fitness with both apparent molecular weight and  $K_{0.5}$  for FBP suggest that the effects of the amino acid substitutions on tetramer formation with the resultant effect on FBP inhibition provide the molecular basis for the improved fitness that is observed with these mutations.

**Effect of *glpK* Mutations on Auto-regulation**—In addition to observing the effects of the mutations on *GlpK* kinetics, we also examined whether the allozymes affect regulation of *glpK* expression. This was examined in isogenic strains that each carry the relevant mutation in the genomic copy of the *glpK* gene in the *E. coli* MG1655 wild type genetic background (4, 5).

**Expression of *glpK***—We measured *glpK* expression in the wild type parent and the four *GlpK* mutant strains during logarithmic growth by quantitative PCR. This revealed that glycerol kinase expression is greatly reduced (13–66% of wild-type expression) in each of the *glpK* mutant strains (Table 3). Reduced *GlpK* expression is also indicated from assays of whole-cell lysates, which show lower *GlpK* activity in *GlpK* mutant strains compared with wild type (supplemental Fig. S2). Reduced expression of *glpK* has previously been associated with loss of FBP sensitivity in *GlpK* mutants (6, 11). Significantly, like reduced FBP sensitivity, reduced *glpK* expression correlates to increased glycerol fitness across the set of strains (Pearson coefficient *r* = -0.98, *p* = 0.003), as shown in Fig. 2D.

***glpK* Mutations Induce Auto-catabolite Repression**—Expression of the *glpFKX* operon is repressed by *GlpR* in absence of intracellular glycerol (specific repression) and by CRP when levels of cAMP are low (catabolite repression). Because *GlpR* repression should be alleviated during growth on glycerol,

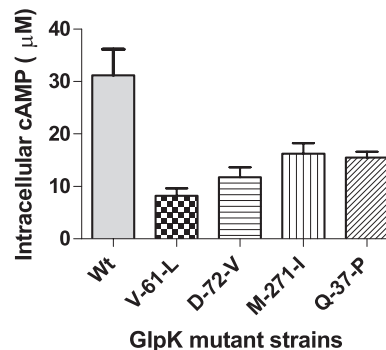


**FIGURE 3. Glycerol kinase mutant strains have reduced intracellular cAMP.** Intracellular cAMP concentrations in four glycerol kinase mutant strains are significantly reduced compared with wild type (*p* = 0.0022, two-tailed one-way ANOVA with Dunnett's post-test). Bars represent average of three independent measurements ± S.D.

repression of *glpFKX* by catabolite repression was suspected. As shown in Fig. 3, intracellular cAMP levels in the four *GlpK* mutant strains are significantly reduced, showing only 30–50% of the amount measured in the wild type strain. Reductions in cAMP levels correlate to both reduced *glpK* expression (Pearson *r* = 0.91, *p* = 0.03) and increased glycerol fitness (Pearson *r* = -0.97, *p* = 0.006, Fig. 2C).

We additionally measured transcription levels of two other genes whose expression is regulated by cAMP levels, aspartate ammonia-lyase (*aspA*), and pyruvate dehydrogenase E1 component (*aceE*) (24). Transcription of one of these genes, *aspA*, changed in a manner strongly consistent with decreased catabolite repression, with loss of expression correlating nearly linearly with observed cAMP reduction (Pearson coefficient *r* = 0.96, *p* = 0.008) and increased glycerol fitness (Pearson *r* = -0.99, *p* = 0.0005) across the *GlpK* mutant strains. Differences in *aceE* transcription between the mutant strains did not correlate well to corresponding differences in fitness or cAMP levels, but was increased in the *GlpK* mutant strains overall compared with wild type, consistent with increased catabolite repression.

Overall, differences in intracellular cAMP levels and transcription of catabolite-regulated genes indicate that the *GlpK* mutants significantly increase auto-catabolite repression during growth on glycerol, and the strong inverse correlation between cAMP levels and fitness suggest the two parameters are related.

**Frequency of *GlpK* Mutations**—To further examine the adaptive plasticity of the *E. coli* genome in response to glycerol media, an additional 44 glycerol-evolved lineages were gener-



## Functional Effects of Adaptive GLPK Mutants in *E. coli*

**TABLE 4**

**Mutation frequency of various GlpK residues acquired from laboratory evolution of 50 total lineages on glycerol minimal medium**

Residue change <sup>a</sup>		No. of lineages
D72	A (13), V (7)	20
M271	I (3)	4
A18	S, T	2
G94	D, G <sup>b</sup>	2
G235	ins. KGG, A	2
Q37P		1
V61L		1
Other mutations acquired by only a single strain <sup>c</sup>		16
No <i>glpK</i> mutation		3
Multiple <i>glpK</i> mutations <sup>d</sup>		1

<sup>a</sup> Residue change is shown with the locus if the locus was only altered in one lineage; otherwise the resulting residues are shown in the second column. If the locus was altered in multiple lineages, the number of times it was altered to a particular residue is given in parentheses. The residue changes examined in detail in this study are shown in bold.

<sup>b</sup> One synonymous mutation discovered, G-94-G, which results from nucleotide change g285a.

<sup>c</sup> Loci of all discovered GlpK mutations in supplemental Table II.

<sup>d</sup> Three different *glpK* mutations were detected in one lineage (eBOP86) (supplemental Table S2). This population harbored competing GlpK mutants in different subpopulations, as confirmed by Sanger sequencing of individual colonies.

ated and screened for mutations in *glpK*, bringing the total number of glycerol-evolved lineages to 50. Single non-synonymous *glpK* mutations were fixed or nearly fixed in 94% (47/50) of the populations (Table 4 and supplemental Table S2), with no single colony isolated harboring more than one *glpK* mutation.

This large collection of strains allows us to examine the relative frequency that mutations fix to various GlpK loci. Most of loci mutated were only fixed in a single lineage, including GlpK V61L and Q37P. Only five codons were repeatedly mutated across multiple lineages, as summarized in Table 4.

The Asp-72 residue was by far the most frequently altered, mutated in 20 of the 50 lineages by substitution of the same nucleotide (*glpK* 218). Asp-72 was altered to valine in 7 lineages and alanine in 13 lineages (Table 4). The extraordinarily high frequency of fixed mutations to the *glpK* 218 locus is too high to be due to preferred selection alone, since the spontaneous mutation rate is too low to account for mutations to this locus even being sampled so consistently within the given adaptation period (supplemental Note S4, estimated binomial pdf  $p = 3E-17$ ). This strongly suggests that the *glpK* 218 allele has an elevated mutation rate.

### DISCUSSION

The aim of this study was to investigate the biochemical mechanism by which adaptive GlpK mutants improve fitness during growth on glycerol in minimal medium. Mutations often alter many enzyme parameters, but most of the parameter effects do not impact fitness. To identify the causal changes we characterized four mutant enzymes to identify changes that correlate to fitness during growth on glycerol (4). Below we interpret these results to develop an improved understanding of GlpK, glycerol metabolism, and the observed adaptation process.

**Structure-Function Analysis of the Variant GlpK Enzymes—GlpK V61L**—The V61L mutant imparts the largest fitness increase during growth on glycerol minimal medium among the four allozymes studied (Table 1), and essentially eliminates

FBP affinity and tetramer formation (Fig. 1C and Table 2). Residue 61 sits within an  $\alpha$ -helix that is critical to tetramer stability. Mutations to two near-by residues (A65T and S58W) have also been shown to disrupt tetramer formation and abolish FBP inhibition (15, 16). This particular residue was only altered in one lineage, but six other lineages acquired mutations within five residues of this locus (supplemental Table S2), and it is likely that they all increase fitness by abolishing FBP inhibition.

**GlpK D72V**—The GlpK D72V mutation is located near the C-terminal end of the same  $\alpha$ -helix impacted by V61L. The carboxylate group of Asp-72 forms a salt bridge with Lys-232, which is in the loop that binds to FBP. A GlpK D72N allozyme has been structurally characterized, and the loss of the carboxyl group was hypothesized to disrupt the electrostatic interactions of the region important to tetramer formation (15). The hydrophobic side chains of both valine and alanine should also significantly disrupt those interactions.

**GlpK M271I**—The widespread effects of this mutant, which significantly reduces the enzyme sensitivity to both FBP and IIA<sup>Glc</sup> and alters its catalytic activity, likely results from the exchanged residue being in the conserved ATPase core. Similar wide-spread effects were observed when a residue that interacts with Met-271 in the ATPase core, Gly-304, was exchanged for serine. This glycine is hydrogen-bonded to the carbonyl oxygen of Met-271 through its backbone amide (25), suggesting these mutations alter many of the same interactions.

The  $V_{max}$  of the M271I enzyme is almost 5-fold higher than wild type GlpK. However, this residue change produces a single observed Michaelis constant instead of the two observed in the native enzyme. This single Michaelis constant is 20-fold higher (250  $\mu$ M) than the native GlpK high affinity constant, suggesting the M271I variant has reduced enzymatic efficiency. This could result in less turnover at low concentrations of ATP, though it is unlikely that this would much impact *in vivo* activity since intracellular ATP concentrations are generally kept much higher (>2 mM) (26) than the reduced affinity constant (0.25 mM, Table 2).

**GlpK Q37P**—Though the GlpK Q37P variant causes the smallest fitness increase among the four GlpK variants examined, it still significantly improves growth on glycerol minimal medium relative to native GlpK ( $\sim 0.06$  h<sup>-1</sup>,  $\sim 20\%$  increase). The altered residue is part of the conserved ATPase catalytic core, on a loop in domain I (27). This loop undergoes a conformational change upon glycerol binding in the glycerol kinase of *Enterococcus casseliflavus*, which has a very similar structure to the *E. coli* enzyme and 78% sequence identity (28). The underlying nucleotide mutation in the *glpK* gene is also within a putative GlpR-binding site (29); however, since GlpR repression is not active during growth on glycerol this is likely not relevant to its selection.

Like the M271I variant, the Q37P variant strongly impacts multiple catalytic properties in addition to FBP inhibition and tetramer dissociation. The mutation causes the largest  $V_{max}$  increase among the variants, though like the M271I mutant, increased velocity is coupled with decreased ATP affinity and enzyme efficiency is only about a quarter of native enzyme. But also like M271I, this decrease likely does not affect activity at *in vivo* ATP concentrations.

**Loss of FBP Affinity and Tetramer Stability**—The primary mechanism used by selection to increase *in vivo* G<sub>l</sub>pK activity appears to be residue changes that decreased tetramer stability and FBP inhibition, which as previously described, are thermodynamically and structurally related. These two parameters are also the most robustly and consistently affected parameters across the examined allozymes, and are the only measured enzymatic parameters that correlate to the measured fitness differences (Table 2). *In vivo*, intracellular FBP has been estimated to be in the 3–5 mM range during growth on glycerol (26), which Fig. 1C indicates imposes near maximum inhibition on wild type G<sub>l</sub>pK. This suggests reduction of FBP inhibition is a potent mechanism for increasing intracellular G<sub>l</sub>pK activity.

While we have not demonstrated that all of the different G<sub>l</sub>pK mutants acquired across the 50 glycerol-adapted lineages increase fitness by reducing FBP sensitivity, it is worth noting that all of the mutated loci (with the exception of Gln-37) are in domains involved in the formation of the tetramer interface of the FBP-binding site. Additionally, G<sub>l</sub>pK mutants with reduced FBP sensitivity have also been repeatedly isolated from screens of mutagenized cells for reduced glucose control and loss of diauxic growth (8, 15). This may indicate that FBP sensitivity is particularly malleable to modulation by mutation. Conversely, the persistence of the highly FBP-sensitive G<sub>l</sub>pK in the wild type, despite the indicated wide availability of variants with reduced sensitivity, suggests that this trait is positively selected even though it reduces growth on glycerol. It may also suggest that the native enzyme specifically retains the ability to quickly relax FBP inhibition in the presence of glycerol (30).

**Catabolite Repression by G<sub>l</sub>pK Mutations**—It is well known that glycerol metabolism partially induces catabolite repression (31–33), but the response observed is much stronger in the G<sub>l</sub>pK mutant strains given that the cAMP levels approach those observed during growth on glucose (supplemental Fig. S3b). Increased glycerol-induced catabolite repression has also been observed in other FBP-desensitized G<sub>l</sub>pK mutants (6), though the underlying mechanism has been a topic of ongoing examination. An initial model posited that IIA<sup>Glc</sup> becomes sequestered by increased expression of G<sub>l</sub>pK in response to glycerol, and that this reduced the levels of phosphorylated IIA<sup>Glc</sup> available to stimulate adenylate cyclase to produce cAMP (31, 33). However, it has since been shown that reduction of cAMP during growth on glycerol is independent of IIA<sup>Glc</sup>, but instead is dependent on glycerol-3-phosphate (G3P), the product of G<sub>l</sub>pK (32).

The results of the study described herein provide no direct evidence to validate either hypothesis, but are more consistent with the G3P-dependent model. If correct, cAMP levels correlate to fitness because both are direct consequences of increased intracellular G<sub>l</sub>pK activity and glycerol metabolism. This would also explain why cAMP levels in the G<sub>l</sub>pK mutant strains are only altered during growth on glycerol and not on other substrates (supplemental Fig. S3b). The results also conflict with the IIA<sup>Glc</sup>-sequestering hypothesis because the G<sub>l</sub>pK mutants do not generally have increased IIA<sup>Glc</sup> affinity (Table 2), and *glpK* expression is reduced in the mutants even though cAMP levels still fall (Table 3, Fig. 3).

**Reduced *glpK* Expression**—Counterintuitively, glycerol fitness appears to increase with decreased G<sub>l</sub>pK expression (Fig. 2D). Reduced cAMP concentrations across the mutant strains suggest that catabolite repression of the *glpFKX* operon is responsible (3, 34). Combined, these results indicate a negative feedback response where accumulation of G3P by G<sub>l</sub>pK activity reduces cAMP synthesis and *glpK* expression until a steady-state between G<sub>l</sub>pK activity and cAMP regulation is reached. The correlation between decreased mutant G<sub>l</sub>pK expression and increased fitness suggests that the cAMP-mediated feedback loop proportionally attenuates rather than completely counteracts total *in vivo* G<sub>l</sub>pK activity gains caused by loss of FBP inhibition.

The existence of a negative feedback mechanism that limits use of a substrate in the absence of alternative carbon sources seems counterproductive to growth. However, loss of both FBP inhibition and catabolite repression of G<sub>l</sub>pK activity have long been known to lead to synthesis of lethal levels of methylglyoxal during growth on glycerol (35–39). Methylglyoxal is synthesized in response to excessive accumulation of dihydroxyacetone phosphate (DHAP) and depletion of free inorganic phosphate, and at subtoxic levels frees inorganic phosphate for downstream metabolic reactions (38–40). Glycerol metabolism is prone to causing methylglyoxal toxicity because it enters glycolysis as DHAP. If catabolite repression is induced by G3P, it would provide a direct mechanism to buffer methylglyoxal toxicity from glycerol metabolism.

**High Frequency of *glpK* 218 Mutations**—The mechanism underlying the increased mutation rate of the *glpK* 218 allele is not known. It may be significant that the wild type adenine allele is a predicted methylation target of Dam methylase. However, while methylated cytosines are well-characterized mutation hotspots (41) (possibly suggesting that the seven 218 a→t mutations were transiently 218 a→c mutations), we have found no published observation of increased mutation rates among methylated adenines or Dam methylase targets. We have also considered the possibility that this hot spot is a transcription-driven mutation, caused by open exposure of the non-coding DNA strand during mRNA synthesis that can particularly affect nucleotides that are unpaired in the majority of available secondary structures (42–44). However, analysis of the local secondary structure of the wild type 218 allele by mfg software (45) indicates it is not frequently unpaired. Additionally, transcription-directed mutations have only been observed following severe nutritional stress while the glycerol-evolved strains were grown with excess substrate.

Although the cause of this hot spot is currently unknown, its existence in a position that significantly increases fitness under a growth condition related to the function of the encoded gene suggests that the site-specific increased mutation rate is itself adaptive. This is not the first indication that mutation hotspots in bacteria may preferentially appear at loci that impart an adaptive function, as a number of other adaptive mutation hotspots have been putatively identified across a wide set of core metabolic genes by comparative analysis of sequenced *E. coli* genomes (46). That study also suggested that these hotspots may exist to facilitate repeated adaptation to transient growth conditions that impose significant trade-offs with more com-



## Functional Effects of Adaptive GlpK Mutants in *E. coli*

mon growth conditions. When applied to glycerol metabolism, this hypothesis suggests that the 218 locus hot spot could exist to accommodate the trade-off between GlpK activity and vulnerability to methylglyoxal toxicity previously described, and/or the observed growth defect of the GlpK mutant strains on sugars ([supplemental Note S3](#)).

The relative fitness relationship between the examined GlpK mutants indicates that at least one GlpK mutant (V61L) exists that can impart a larger fitness increase than D72V. This raises the question of why the increased mutation rate is not applied to the nucleotide coding the most adaptive GlpK mutant if this hot spot exists to facilitate glycerol adaptation. This question cannot be addressed before more is known about the mechanism underlying the increased mutation rate, as it is possible that nucleotide 218 is in a better position to become a hot spot due to nucleotide sequence properties rather than impact on enzyme activity and fitness. However, it is also possible that *glpK* 218 is the acquired hotspot because its mutation increases fitness more reliably, due to the cumulative effect of all the possible mutants accessible from this locus, or due to the robustness of the resulting mutants to epistatic interactions with adaptive mutations in other genes. It is becoming increasingly apparent that epistatic interactions frequently occur between adaptive mutations (47–49) even when the affected genes have unrelated functions (50, 51). In this case, the only strain in which the V61L mutant appeared included a large-scale duplication, and was among the fewer than 20% of lineages that did not acquire a mutation to either RNA polymerase gene *rpoB* or *rpoC* (5, 52). This suggests that while the V61L mutant is more advantageous than the D72V mutant in an otherwise wild type genetic background, it may have less favorable epistatic interactions with frequently co-acquired mutants that could make it a less effective hotspot target than GlpK Asp-72 mutants in an adapting genome. For instance, evidence of positive epistatic interactions between GlpK D72V and *rpoC* mutations has already been found (4).

**The Study of Adaptive Constraints**—In this study we have attempted to determine the molecular mechanism underlying an enzyme adaption by identifying properties that are altered in a manner that correlates to the ability of the mutations to increase fitness. The underlying assumption has been that mutations to the same gene improve growth by alleviating the same constraint. We are able to show that rate-limiting GlpK activity is increased by reducing tetramer stability and FBP inhibition, and that this is the mechanism likely used by the majority of GlpK mutants acquired by this selection process. We additionally show how the effects of the mutations are attenuated by negative feedback regulation, which provides further support that G3P rather than IIA<sup>Glc</sup> mediates glycerol-induced catabolite repression. We also found evidence that the most frequently acquired mutant is the result of a mutation hotspot, which may exist to facilitate rapid metabolic optimization when glycerol is sole available carbon source.

Currently, study of adaptive constraints at the molecular level has mostly been limited to directed protein evolution studies that have examined how mutations selected to alter specific enzyme properties achieve that effect (49, 53–59). This is one of a handful of studies to date to examine the molecular

basis underlying the effect of a set of adaptive mutations to the same gene on organism fitness (2, 60, 61).

However, even though many adaptive mutations are now being discovered from the growing number of laboratory evolution studies that utilize gene and genome resequencing (5, 62–68), it may not be feasible to determine the constraints underlying many of them. For instance, it may not be accurate in all cases to assume that mutations to the same gene alleviate the same constraint or do so by the same mechanism. Additionally, replicate lineages may alleviate the same constraint through modification of different genes. This approach can also be very technically difficult since it requires both very sensitive measurements of fitness as well as assays of multiple enzyme properties, regulatory mechanisms, and potential pathway- or network-wide effects across a number of different mutants. Many of these problems are likely to be more significant for adaptations to genes that are not very well characterized, or have many interactions or functions, such as mutations to global regulatory proteins that are frequently being discovered in laboratory adaptations (52, 68–72).

In this study many of these difficulties were simplified because the subject was a metabolic enzyme that has already been well-characterized. Even so, we were unable to account for one effect the mutants had on phenotype, reduced growth rate on glycolytic substrates ([supplemental Fig. S3 and Note S3](#)), largely because this effect most likely results from a previously unrecognized interaction.

This perhaps underlies the point that while studying constraints and adaptive processes is technically challenging, they also hold great potential for discovering new and important interactions. Identifying the constraints that define growth potential and drive the adaptive processes will be critical to developing a comprehensive understanding of biochemical networks and systems biology.

---

*Acknowledgments*—We thank Milton Saier for generous time and feedback, Young Seoub Park, and Dae Hee Lee for invaluable technical advice, Megan Anderson (Quake Lab, Stanford University) for sharing GlpK cloning constructs, Jessica Na, Pamela S. Miller, and Tzu-Wen Huang for expert technical assistance, and Jan Schellenberger and Nate Lewis for statistical advice.

---

## REFERENCES

1. Fong, S. S., Joyce, A. R., and Palsson, B. Ø. (2005) *Genome Research* **15**, 1365–1372
2. Knight, C. G., Zitzmann, N., Prabhakar, S., Antrobus, R., Dwek, R., Hebestreit, H., and Rainey, P. B. (2006) *Nat. Genet.* **38**, 1015–1022
3. Lin, E. C. (1976) *Annu. Rev. Microbiol.* **30**, 535–578
4. Applebee, M. K., Herrgård, M. J., and Palsson, B. Ø. (2008) *J. Bacteriol.* **190**, 5087–5094
5. Herring, C. D., Raghunathan, A., Honisch, C., Patel, T., Applebee, M. K., Joyce, A. R., Albert, T. J., Blattner, F. R., van den Boom, D., Cantor, C. R., and Palsson, B. Ø. (2006) *Nat. Genet.* **38**, 1406–1412
6. Zwaig, N., Kistler, W. S., and Lin, E. C. (1970) *J. Bacteriol.* **102**, 753–759
7. Pettigrew, D. W., Yu, G. J., and Liu, Y. (1990) *Biochemistry* **29**, 8620–8627
8. Zwaig, N., and Lin, E. C. (1966) *Science* **153**, 755–757
9. Postma, P. W., Epstein, W., Schuitema, A. R., and Nelson, S. O. (1984) *J. Bacteriol.* **158**, 351–353
10. Novotny, M. J., Frederickson, W. L., Waygood, E. B., and Saier, M. H., Jr. (1985) *J. Bacteriol.* **162**, 810–816

11. Holtman, C. K., Pawlyk, A. C., Meadow, N. D., and Pettigrew, D. W. (2001) *J. Bacteriol.* **183**, 3336–3344
12. de Riel, J. K., and Paulus, H. (1978) *Biochemistry* **17**, 5141–5146
13. de Riel, J. K., and Paulus, H. (1978) *Biochemistry* **17**, 5134–5140
14. Yu, P., and Pettigrew, D. W. (2003) *Biochemistry* **42**, 4243–4252
15. Liu, W. Z., Faber, R., Feese, M., Remington, S. J., and Pettigrew, D. W. (1994) *Biochemistry* **33**, 10120–10126
16. Bystrom, C. E., Pettigrew, D. W., Branchaud, B. P., O'Brien, P., and Remington, S. J. (1999) *Biochemistry* **38**, 3508–3518
17. Herring, C. D., Glasner, J. D., and Blattner, F. R. (2003) *Gene* **311**, 153–163
18. Pettigrew, D. W. (2009) *Arch Biochem. Biophys.* **492**, 29–39
19. Death, A., and Ferenci, T. (1994) *J. Bacteriol.* **176**, 5101–5107
20. Lee, D. H., and Palsson, B. O. (2010) *Appl. Env. Microbiol.* **76**, 4158–4168
21. Covert, M. W., Knight, E. M., Reed, J. L., Herrgard, M. J., and Palsson, B. O. (2004) *Nature* **429**, 92–96
22. Muller, P. Y., Janovjak, H., Miserez, A. R., and Dobbie, Z. (2002) *BioTechniques* **32**, 1372–1374, 1376, 1378–1379
23. Ibarra, R. U., Edwards, J. S., and Palsson, B. O. (2002) *Nature* **420**, 186–189
24. Gosset, G., Zhang, Z., Nayyar, S., Cuevas, W. A., and Saier, M. H., Jr. (2004) *J. Bacteriol.* **186**, 3516–3524
25. Pettigrew, D. W., Liu, W. Z., Holmes, C., Meadow, N. D., and Roseman, S. (1996) *J. Bacteriol.* **178**, 2846–2852
26. Bennett, B. D., Kimball, E. H., Gao, M., Osterhout, R., Van Dien, S. J., and Rabinowitz, J. D. (2009) *Nat. Chem. Biol.* **5**, 593–599
27. Hurley, J. H., Faber, H. R., Worthylake, D., Meadow, N. D., Roseman, S., Pettigrew, D. W., and Remington, S. J. (1993) *Science* **259**, 673–677
28. Yeh, J. I., Charrier, V., Paulo, J., Hou, L., Darbon, E., Claiborne, A., Hol, W. G., and Deutscher, J. (2004) *Biochemistry* **43**, 362–373
29. Weissenborn, D. L., Wittekindt, N., and Larson, T. J. (1992) *J. Biol. Chem.* **267**, 6122–6131
30. Camps, M., Herman, A., Loh, E., and Loeb, L. A. (2007) *Crit. Rev. Biochem. Mol. Biol.* **42**, 313–326
31. Chagneau, C., Heyde, M., Alonso, S., Portalier, R., and Laloi, P. (2001) *J. Bacteriol.* **183**, 5675–5683
32. Eppler, T., Postma, P., Schütz, A., Völker, U., and Boos, W. (2002) *J. Bacteriol.* **184**, 3044–3052
33. Rohwer, J. M., Bader, R., Westerhoff, H. V., and Postma, P. W. (1998) *Mol. Microbiol.* **29**, 641–652
34. Keseler, I. M., Bonavides-Martínez, C., Collado-Vides, J., Gama-Castro, S., Gunsalus, R. P., Johnson, D. A., Krummenacker, M., Nolan, L. M., Paley, S., Paulsen, I. T., Peralta-Gil, M., Santos-Zavaleta, A., Shearer, A. G., and Karp, P. D. (2009) *Nucleic Acids Res.* **37**, D464–470
35. Freedberg, W. B., Kistler, W. S., and Lin, E. C. (1971) *J. Bacteriol.* **108**, 137–144
36. Krymkiewicz, N., Diéguez, E., Rekarte, U. D., and Zwaig, N. (1971) *J. Bacteriol.* **108**, 1338–1347
37. Zhu, M. M., Skraly, F. A., and Cameron, D. C. (2001) *Metab. Eng.* **3**, 218–225
38. Booth, I. R. (2005) *Module 3.4.3 Glycerol and Methylglyoxal Metabolism, Escherichia coli and Salmonella*, Online Ed., ASM Press, Washington, D.C.
39. Cooper, R. A. (1984) *Annu. Rev. Microbiol.* **38**, 49–68
40. Ferguson, G. P., Töttemeyer, S., MacLean, M. J., and Booth, I. R. (1998) *Arch. Microbiol.* **170**, 209–218
41. Lutsenko, E., and Bhagwat, A. S. (1999) *Mutat. Res.* **437**, 11–20
42. Foster, P. L. (2007) *Crit. Rev. Biochem. Mol. Biol.* **42**, 373–397
43. Wright, B. E. (2004) *Mol. Microbiol.* **52**, 643–650
44. Burkala, E., Reimers, J. M., Schmidt, K. H., Davis, N., Wei, P., and Wright, B. E. (2007) *Microbiology* **153**, 2180–2189
45. Wright, B. E., Reschke, D. K., Schmidt, K. H., Reimers, J. M., and Knight, W. (2003) *Mol. Microbiol.* **48**, 429–441
46. Chattopadhyay, S., Weissman, S. J., Minin, V. N., Russo, T. A., Dykhuizen, D. E., and Sokurenko, E. V. (2009) *Proc. Natl. Acad. Sci. U.S.A.* **106**, 12412–12417
47. Le Gac, M., and Doebeli, M. (2010) *Mol. Ecol.* **19**, 2430–2438
48. MacLean, R. C., Perron, G. G., and Gardner, A. (2010) *Genetics* **186**, 1345–1354
49. Weinreich, D. M., Delaney, N. F., Depristo, M. A., and Hartl, D. L. (2006) *Science* **312**, 111–114
50. He, X., Qian, W., Wang, Z., Li, Y., and Zhang, J. (2010) *Nat. Genet.* **42**, 272–276
51. Cooper, T. F., Remold, S. K., Lenski, R. E., and Schneider, D. (2008) *PLoS Genet.* **4**, e35
52. Conrad, T. M., Frazier, M., Joyce, A. R., Cho, B. K., Knight, E. M., Lewis, N. E., Landick, R., and Palsson, B. Ø. (2010) *Proc. Natl. Acad. Sci. U.S.A.* **107**, 20500–20505
53. Aponte, R. A., Zimmermann, S., and Reinstein, J. (2010) *J. Mol. Biol.* **399**, 154–167
54. Miller, S. P., Lunzer, M., and Dean, A. M. (2006) *Science* **314**, 458–461
55. Couñago, R., Chen, S., and Shamoo, Y. (2006) *Mol Cell* **22**, 441–449
56. Couñago, R., Wilson, C. J., Peña, M. I., Wittung-Stafshede, P., and Shamoo, Y. (2008) *Protein Eng. Des. Sel.* **21**, 19–27
57. DePristo, M. A., Weinreich, D. M., and Hartl, D. L. (2005) *Nat. Rev. Genet.* **6**, 678–687
58. Bokma, E., Koronakis, E., Lobedanz, S., Hughes, C., and Koronakis, V. (2006) *FEBS Lett.* **580**, 5339–5343
59. Tomatis, P. E., Fabiane, S. M., Simona, F., Carloni, P., Sutton, B. J., and Vila, A. J. (2008) *Proc. Natl. Acad. Sci. U.S.A.* **105**, 20605–20610
60. Crozat, E., Winkworth, C., Gaffé, J., Hallin, P. F., Riley, M. A., Lenski, R. E., and Schneider, D. (2010) *Mol. Biol. Evol.* **27**, 2113–2128
61. Giraud, A., Arous, S., De Paepé, M., Gaboriau-Routhiau, V., Bambou, J. C., Rakotobe, S., Lindner, A. B., Taddei, F., and Cerf-Bensussan, N. (2008) *PLoS Genet.* **4**, -
62. Hegreness, M., and Kishony, R. (2007) *Genome Biol.* **8**, 201
63. Conrad, T. M., Joyce, A. R., Applebee, M. K., Barrett, C. L., Xie, B., Gao, Y., and Palsson, B. Ø. (2009) *Genome Biol.* **10**, R118
64. Charusanti, P., Conrad, T. M., Knight, E. M., Venkataraman, K., Fong, N. L., Xie, B., Gao, Y., and Palsson, B. Ø. (2010) *PLoS Genet.* **6**, e1001186
65. Sota, M., Yano, H., Hughes, J. M., Daughdrill, G. W., Abdo, Z., Forney, L. J., and Top, E. M. (2010) *ISME J* **4**, 1568–1580
66. Cooper, V. S., Schneider, D., Blot, M., and Lenski, R. E. (2001) *J. Bacteriol.* **183**, 2834–2841
67. Woods, R., Schneider, D., Winkworth, C. L., Riley, M. A., and Lenski, R. E. (2006) *Proc. Natl. Acad. Sci. U.S.A.* **103**, 9107–9112
68. Cooper, T. F., Rozen, D. E., and Lenski, R. E. (2003) *Proc. Natl. Acad. Sci. U.S.A.* **100**, 1072–1077
69. Philippe, N., Crozat, E., Lenski, R. E., and Schneider, D. (2007) *Bioessays* **29**, 846–860
70. Maharjan, R., Seeto, S., Notley-McRobb, L., and Ferenci, T. (2006) *Science* **313**, 514–517
71. Crozat, E., Philippe, N., Lenski, R. E., Geiselmann, J., and Schneider, D. (2005) *Genetics* **169**, 523–532
72. Wilson, J. W., Ott, C. M., Höner, zu Bentrup, K., Ramamurthy, R., Quick, L., Porwollik, S., Cheng, P., McClelland, M., Tsaprilis, G., Radabaugh, T., Hunt, A., Fernandez, D., Richter, E., Shah, M., Kilcoyne, M., Joshi, L., Neiman-Gonzalez, M., Hing, S., Parra, M., Dumars, P., Norwood, K., Bober, R., Devich, J., Ruggles, A., Goulart, C., Rupert, M., Stodieck, L., Stafford, P., Catella, L., Schurr, M. J., Buchanan, K., Morici, L., McCracken, J., Allen, P., Baker-Coleman, C., Hammond, T., Vogel, J., Nelson, R., Pierson, D. L., Stefanyshyn-Piper, H. M., and Nickerson, C. A. (2007) *Proc. Natl. Acad. Sci. U.S.A.* **104**, 16299–16304
73. Larson, T. J., Ye, S. Z., Weissenborn, D. L., Hoffmann, H. J., and Schweizer, H. (1987) *J. Biol. Chem.* **262**, 15869–15874